Geophysical investigation of glass 'hotspots' in glass dumps as potential secondary raw material sources

Mutafela, Richard Nasilele; Lopez, Etzar Gomez; Dahlin, Torleif; Kaczala, Fabio; Marques, Marcia; Jani, Yahya; Hogland, William

Published in:
Waste Management

DOI:
10.1016/j.wasman.2020.03.027

2020

Document Version:
Publisher's PDF, also known as Version of record

Waste Management 106 (2020) 213–225

Contents lists available at ScienceDirect

Waste Management

journal homepage: www.elsevier.com/locate/wasman

Geophysical investigation of glass 'hotspots' in glass dumps as potential secondary raw material sources

Richard Nasilele Mutafela [a,*], Etzar Gomez Lopez [b], Torleif Dahlin [b], Fabio Kaczala [c], Marcia Marques [a,d], Yahya Jani [a], William Hogland [a]

[a] Department of Biology & Environmental Science, Faculty of Health and Life Sciences, Linnaeus University, SE-391 82 Kalmar, Sweden
[b] Division of Engineering Geology, Lund University, P.O. Box 118, SE-221 00 Lund, Sweden
[c] Sweco Environment AB, SE-392 35 Kalmar, Sweden
[d] Department of Sanitary and Environmental Engineering, Rio de Janeiro State University UERJ, R. São Francisco Xavier, 524, CEP 20551-013, Rio de Janeiro, Brazil

ARTICLE INFO

Article history:
Received 8 July 2019
Revised 31 January 2020
Accepted 18 March 2020

Keywords:
Electrical resistivity tomography
Secondary resources
Glass waste
Landfill mining
Waste characterisation
Circular economy

ABSTRACT

This study investigates the potential for Electrical Resistivity Tomography (ERT) to detect buried glass 'hotspots' in a glass waste dump based on results from an open glass dump investigated initially. This detection potential is vital for excavation and later use of buried materials as secondary resources. After ERT, test pits (TPs) were excavated around suspected glass hotspots and physico-chemical characterisation of the materials was done. Hotspots were successfully identified as regions of high resistivity (>8000 Ωm) and were thus confirmed by TPs which indicated mean glass composition of 87.2% among samples (up to 99% in some). However, high discrepancies in material resistivities increased the risk for introduction of artefacts, thus increasing the degree of uncertainty with depth, whereas similarities in resistivity between granite bedrock and crystal glass presented data misinterpretation risks. Nevertheless, suitable survey design, careful field procedures and caution exercised by basing data interpretations primarily on TP excavation observations generated good results particularly for near-surface materials, which is useful since glass waste dumps are inherently shallow. Thus, ERT could be a useful technique for obtaining more homogeneous excavated glass and other materials for use as secondary resources in metal extraction and other waste recycling techniques while eliminating complicated and often costly waste sorting needs.

1. Introduction

The world population has been increasing together with resource consumption and waste generation, resulting in negative environmental impacts. It is projected to further increase to 9.8 billion by 2050, which is expected to triple the current resource demand to 140 billion tonnes of minerals, ores, fossil fuels and biomass per year (UN, 2017; UNEP, 2011). Decoupling of the economic growth rate from this high rate of natural resource consumption is thus recommended. In case of metals production, decrease in ore grades and stocks have been reported due to the need to meet the global demand (UNEP, 2013). Some trace elements such as Sb, As, Cd and Pb have been identified as high supply risk due to their low recycling rates, limited number of substitutes and being almost exclusively mined as by-product metals (British Geological Survey, 2015). The growing calls for secondary raw materials and reduced mining will further drop the supply of such elements. Therefore, alternative and sustainable sources are required.

Around former glass factories in south-eastern Sweden, glass dumps are highly contaminated with As, Cd, Pb and Sb, with an estimation of 420,000 m^3 of contaminated materials (420 tonnes of As, 30 tons of Cd and 3100 tons of Pb) in 22 dumps (Höglund et al., 2007). These materials pose contamination risks to humans and the environment (Augustsson et al., 2016), hence they have been recommended for remediation (Hogland et al., 2010). Alsterfors glass waste dump (current study site), for example, has an infiltration rate to groundwater of about 1200 m^3 per year and combined As, B, Cd, Pb and Sb leakages to the Alsterån River at more than 20 kg per year (Höglund et al., 2007). These materials, on the other hand, could potentially contribute as secondary sources of some of the high supply risk metals. High contamination of excavated wastes is one of the main obstacles to their recycling as secondary raw materials (Hull et al., 2005), resulting in

* Corresponding author at: Department of Biology & Environmental Science, Faculty of Health and Life Sciences, Linnaeus University, Stuvaregatan 2, SE-392 31 Kalmar, Sweden.
E-mail address: richardnasilele.mutafela@lnu.se (R.N. Mutafela).

https://doi.org/10.1016/j.wasman.2020.03.027
0956-053X/

preference of landfilling as the only environmentally feasible and safe alternative (Höglund et al., 2007; Jani and Hogland, 2014). However, recent studies have shown the potential to extract these elements from such glass waste with high efficiency, both as a decontamination measure and as future secondary raw materials (Jani and Hogland, 2017, 2018). Since valorisation processes of waste to secondary raw materials have specific quality demands and limits for non-glass materials (Beerkens et al., 2010), obtaining a 'clean' glass waste is important. This is a big challenge because during the on-going remedial excavations of some of the sites in the region, glass gets mixed with other waste fractions, further presenting sorting challenges (Mutafela et al., 2018). It is hereby hypothesized that in some dump sections there exist regions of 'clean' glass (with little or no other material fractions mixed). It is further hypothesized that it could be possible to identify these glass 'hotspots' prior to excavations, which could be carefully excavated to avoid mixing of this glass with the other materials, thus obtain a more homogeneous glass fraction for metal extraction processes.

Geophysical methods could contribute to such an investigation, as they are known for their usefulness in locating subsurface features like buried wastes, whose volumes can later be estimated (Bernstone et al., 2000). They have been used in landfill investigation procedures (such as drilling of boreholes for groundwater monitoring) as a pre-investigation technique aimed at providing valuable information about waste locations, which helps in drilling grid designs and thus aid to rationalize drilling costs (Zarroca et al., 2015; Dumont et al., 2017). Electrical Resistivity Tomography (ERT) in particular can investigate shallow subsurface electrical structures in various environments. Thus based on resistivity differences among dumped materials, glass hotspots can potentially be identified and quantified faster, cheaper and without well-drilling or trench-digging, using such a non-destructive method (Hsu, et al., 2010). Previously, the method has been successfully conducted in various landfill and waste dump studies (Bernstone et al., 2000; Pomposiello et al., 2012; Çınar et al., 2015; Abdulrahman et al., 2016; Dumont et al., 2017), although no such study in a glass waste dump is documented. The success of the method in old glass dumps would potentially result in well-coordinated excavation activities and obtaining of more homogeneous glass waste for metal extraction and other recycling processes.

This study, therefore, aimed to investigate the potential for ERT to map glass hotspots for future metal recovery. The investigation was coupled with digging of verification test pits (TPs) to identify materials registering different resistivities. The study also aimed at characterising physico-chemical properties of the excavated hotspot materials, since waste management and resource recovery cannot be planned and implemented well in the absence of accurate and reliable waste composition data (Edjabou et al., 2015).

2. Materials and methods

2.1. Study sites

The study was conducted at Alsterfors glass factory dumpsite and Madesjö glass waste dump, both located in south-eastern Sweden as shown in Fig. 1.

2.1.1. Madesjö glass waste dump

This dump is located in Nybro Municipality in a moraine region with granite bedrock and a shallow soil depth estimated at 3–5 m (SGU, 2019). Open dumping at the site started with municipal solid waste (MSW) in 1960 until 1969 when mostly crushed glass with some demolition waste from Orrefors glass factory began to be

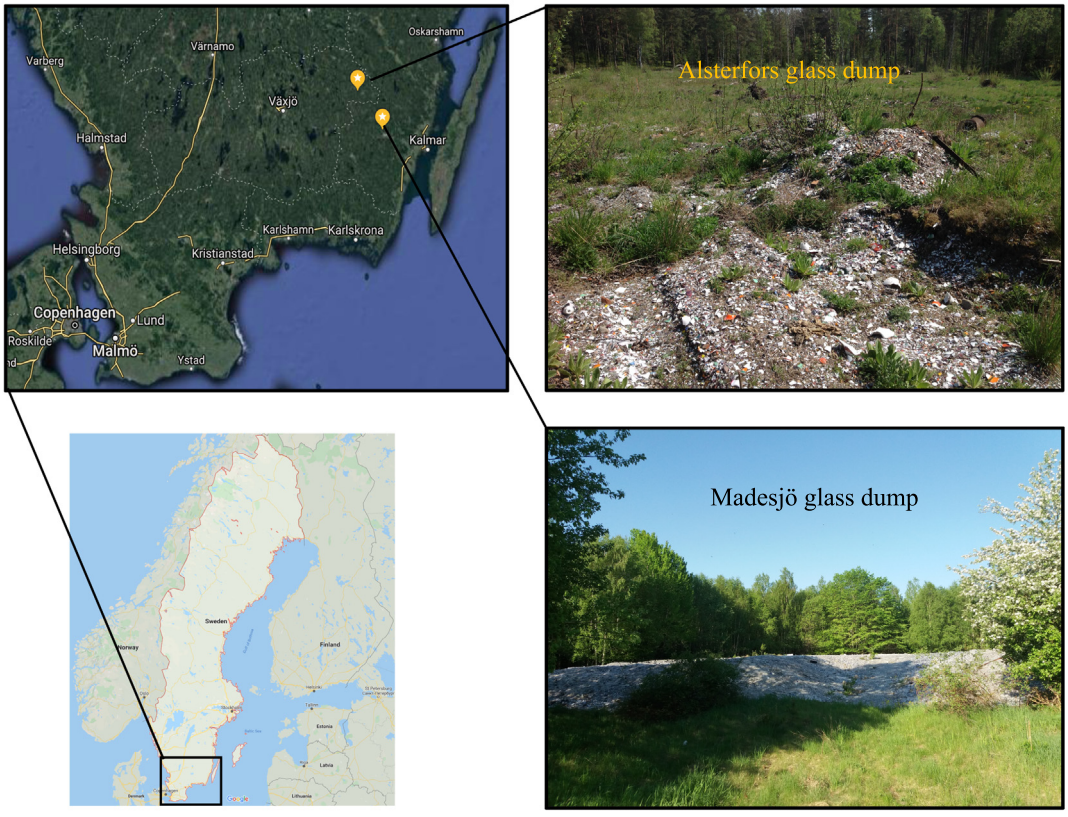

Fig. 1. Alsterfors and Madesjö glass dumps in south-eastern Sweden (Map data ©2020 Google).

dumped there (Länsstyrelsen Kalmar, 2012). Orrefors crystal glass typically constituted SiO_2 (55%), Pb_3O_4 (30′%), K_2CO_3 (13%) and other ingredients (2%) such as As_2O_3 (Duncan, 1995), although glass in the area generally constituted 55–85% SiO_2 (Hermelin and Welander, 1986). Covering approximately 38,500 m^2, Madesjö dumpsite has a small stream on its southern part flowing westward and another on its north-western part flowing south-west, and thus it is designated as a high-risk site (Länsstyrelsen Kalmar, 2019; SGU, 2019).

2.1.2. Alsterfors glass factory dumpsite

Alsterfors glass factory site, with about 4200 m^2 surface area, is situated along the Alsterån River in Uppvidinge Municipality. Geologically, it is located in a moraine region with granite as the main underlying bedrock and an estimated soil depth of 3–10 m (SGU, 2019). The factory was active between 1886 and 1980 and produced different glass types (packaging glass, fibre glass and art glass). Glass factory raw materials were mainly quartz and feldspar sand (SiO_2), soda ($NaCO_3$), potash (K_2O_3), calcite ($CaCO_3$), dolomite ($MgCO_3.CaCO_3$), witherite ($BaCO_3$) and different metal oxides such as Pb_3O_4 and As_2O_3 (Hermelin and Welander, 1986; Uddh-Söderberg et al., 2019). Factory waste (crushed glass, discarded raw material batches, furnace and demolition waste, grinding and acid sludges, etc.) was mostly dumped around the factory premises (Uddh-Söderberg et al., 2019), resulting in a 2600 m^2 dump with approximately 5200 m^3 of glass and other wastes (Höglund et al., 2007), some of which is exposed on the surface. The site is also designated as high-risk and ranked fourth out of thirty nine high-risk objects in the county (Länsstyrelsen Kronoberg, 2018).

2.2. Electrical resistivity Tomography (ERT) surveys

ERT was the geophysical method used in this study. The 2D resistivity method measures and maps electrical resistivity of subsurface materials at different depths along a survey line (Loke et al., 2010; Reynolds, 2011) based on the principle of different materials having different electrical properties naturally (Wang et al., 2015). Electrodes are deployed on a site and connected to a set of multi-electrode cables arranged along a line. Electric current is transmitted through a sequence of different pairs of the deployed electrodes while measuring the resulting potential differences between one or several pairs of electrodes simultaneously. Pulses of direct current (DC) with alternating polarity or low-frequency alternating current (AC) are used (Powers et al., 1999).

In this study, an ABEM Terrameter LS, which is a multi-channel resistivity-IP (Induced Polarisation) instrument, was used together with an Electrode Selector ES10-64C and a set of multi-core electrode cables. The surveys were made using separated electrode cable spreads for current transmission and potential measurement in order to reduce capacitive coupling in the cables, which was expected due to very high resistive surface layers known from previous tests at the sites (Mutafela et al., 2018), in order to optimise the data quality (Dahlin and Leroux, 2012). Two electrode cables were connected to the Terrameter and two to the Electrode Selector, with every other electrode connected to each, as shown in the sketch in Fig. 2a.

Eighty-two stainless steel electrodes were inserted into the ground with an inter-electrode spacing of 1 m. The small spacing was used in order to achieve good horizontal and vertical resolution of the images for a site as shallow as Alsterfors dumpsite (Dahlin and Zhou, 2004; Höglund et al., 2007). The electrode configuration was multiple gradient array (Dahlin and Zhou, 2006). Three lines at Alsterfors (AL_1, AL_2 and AL_3) and two at Madesjö (ML_1 and ML_2) were thus obtained. Fig. 2b and c show equipment set-up at the two sites. Since these ERT surveys in a glass dump were first to the knowledge of the authors, different instrument modes and settings were tried to reach optimum settings as shown in Table 1. At Madesjö, electrode contact resistance was particularly high since it's a glass heap (exposed materials), whereas Alsterfors has soil cover (buried materials). Therefore, in order to reduce electrode contact resistance and transmit sufficient current for good signal strength, ground contact was improved using a gel based on Johnson Revert Optimum around the electrode and in some cases also by adding an extra electrode. The lines obtained at each site were visualised as 2D resistivity images after data processing and inversion (as described in Section 2.4.3), which were used in planning and setting TP excavations.

2.3. Excavation and sampling procedure

Test pits (TPs) were excavated along the profile lines using a 5-tonne excavator, and according to a procedure from Kaczala et al. (2017) where excavated materials were separately stockpiled from each 1 m depth interval. At Alsterfors, twelve TPs were excavated, eleven of which were 2–2.5 m deep and one was 4.5 m deep (on AL_2), whereas at Madesjö eight TPs were excavated at 1.5 m maximum depth due to unstable surface (glass waste). Identified hotspot stockpiles at Alsterfors were later sampled according to the Nordtest Method NT ENVIR 004-1996/05, in order to assess material composition and physico-chemical properties. Thus, four hotspot stockpiles (S1, S2, S3 and S4) were sampled (about 100 kg each) from Alsterfors for analysis. After sampling, stockpiled materials in each case were returned into their respective TPs to restore the site as much as possible.

2.4. Physico-chemical characterisation of hotspot materials

2.4.1. Sample sieving and hand-sorting

To achieve particle size distribution (PSD), the collected samples were sieved using eight sieves (Tidbecks Sweden and Giuliani Technologies) with mesh sizes 63 mm, 31.5 mm, 20 mm, 16 mm, 11.3 mm, 8 mm, 4 mm and 2 mm mounted on a laboratory sieve shaker (Pascall Engineering). Based on particle sizes, the sieved materials were aggregated into course (>31.5 mm), medium (11.3–31.5 mm) and fine (<11.3 mm) fractions. Furthermore, the particle sizes were assessed based on mass percentage of the particles passing through each sieve size. For waste composition, the sieved materials were hand-sorted and the materials fractions categorised into glass, demolition (mainly bricks), soil, organic and residual (plastics, metals, roofing material parts, etc). All fractions sized 2–8 mm were hand-sorted using magnifying lenses while the fractions <2 mm were too fine to hand-sort. All calculations were done on wet weight basis in all instances.

2.4.2. Trace elements and moisture contents

A portable X-Ray Fluorescence (XRF) analyser, Olympus DS-4000 (Innov-X), was used to analyse trace element contents of all samples (oven-dried) below 8 mm. The analysis was done on the hand-sorted glass fraction only and in triplicates in each case. Analysis on the glass fraction was aimed at assessing trace elements potential for future recycling. Sample moisture content was analysed based on dry residue of the fine fraction (FF) of Alsterfors soil samples, Alsterfors glass hotspot samples and Madesjö glass samples according to the Swedish Standard SS-EN 14346:2007.

2.4.3. Data analysis and interpretation

2.4.3.1. ERT profiles. Inversion: The contact resistances were exceptionally high for the Madesjö ERT lines, ranging to over 100,000 Ωm with a mean of 86,000–98,000 Ωm (Table 1), despite the efforts at improving electrode contact. For Alsterfors, the resistances ranged up to 10,000 Ωm with a mean of a few thousand

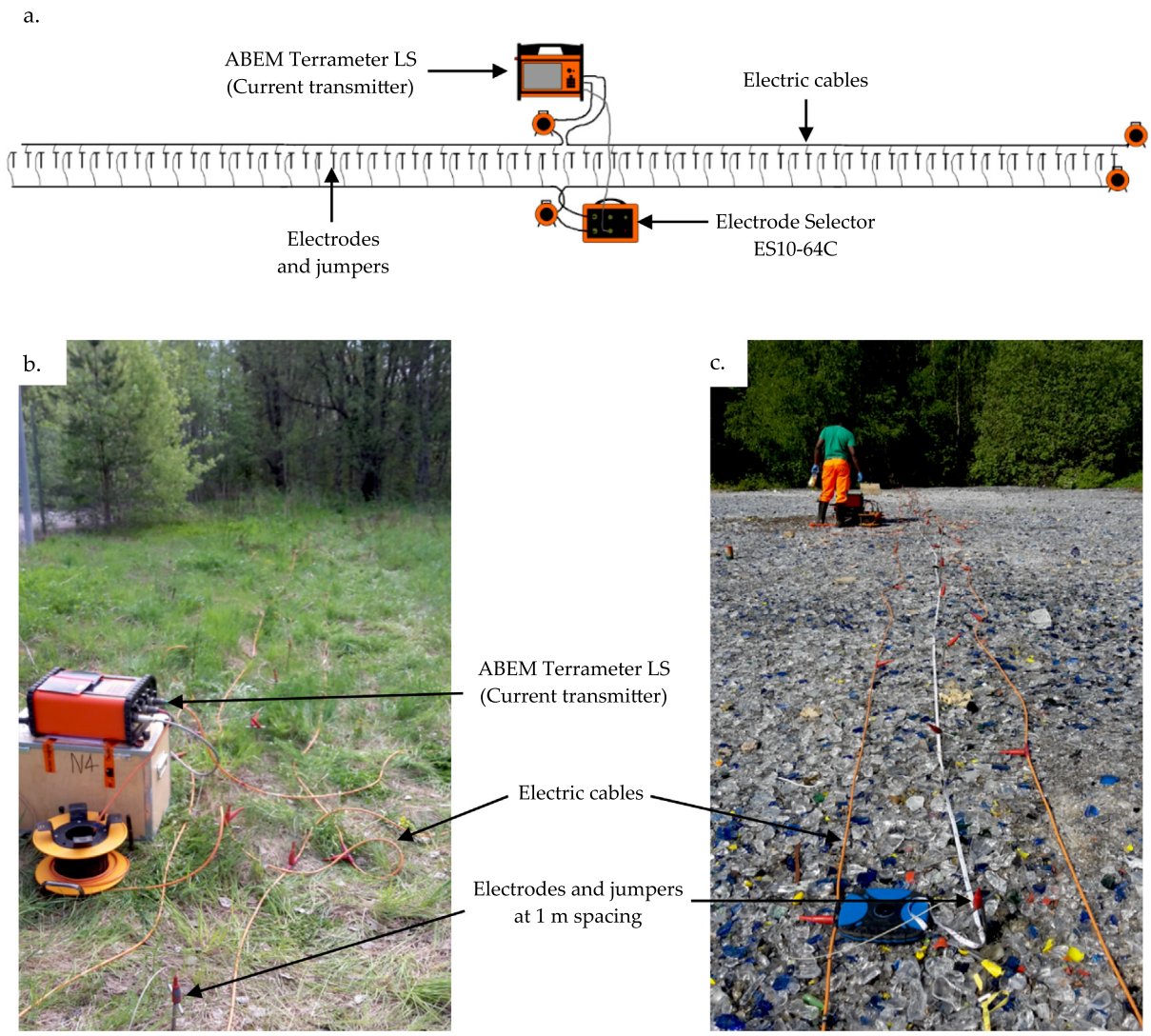

Fig. 2. (a) Sketch of separated electrode cable spreads used for the survey, and cables and electrodes setup along profile lines at (b) Alsterfors and (c) Madesjö.

Table 1
Settings of the different ERT profile lines.

Parameter	AL_1	AL_2	AL_3	ML_1	ML_2
Length (m)	80	80	40	80	55
Electrode separation (m)	1	1	1	1	1
Mean contact resistance (ohm)	2990	4010	2600	85,500	98,300
Coeff. of variance of contact resistance (%)	63.1	62.7	61.8	96.4	98.8
Pulse duration (s)	2.6	2.6	2.6	2.6	2.6
Average current (mA)	102	67	104	11	5
Average variance (%)	0.13	0.18	0.14	0.59	0.81
No. of stacking in data acquisition	6	6	6	6	6
No. of data acquired	1603	1603	833	1547	829
No. of data inverted	1603	1603	833	1532	818
No. of iterations	14	13	17	3	4
No. of layers	15	15	10	15	13
No. of blocks	1215	1215	410	1215	767
Vertical to horizontal flatness ratio	0.5	0.5	0.5	1	1
Width of the model cells (m)	0.5	0.5	0.5	0.5	0.5
Resistivity mean residual (%)	3.0	5.0	3.5	10.5	11.1

Ωm. Nevertheless, the ERT provided consistent apparent resistivity pseudo sections with very few data outliers, which is a sign of good data quality. After removal of a few noisy data points for two of the lines (Table 1), true subsurface resistivity distributions were estimated using the robust inversion (L1 norm) option which is better at handling large contrasts in the resistivities than the least-squares (L2 norm) optimisation method (Loke et al., 2003). The resistivity inversion procedure was achieved using the inversion software RES2DINV (Loke, 1999), which calculates the most likely distribution of resistivity (Çınar et al., 2015).

Interpretation: For both dumps, interpretation of the results was based on TP excavations as well as resistivity values of some materials common in landfill and dump environments as presented in Table 2. For buried glass hotspots in particular, interpretation was also based on the findings from Madesjö open glass dump.

3-D resistivity visualisation (fence diagrams): Cross-sections of the lines on each site were combined using the software EriViz 1.0 (Lund University) to generate three-dimensional (3-D) resistivity profile images known as fence diagrams. Although fence diagrams do not give a full picture of the whole dump, they are advantageous enough to just gather profile images without using interpolation which may add artefacts (Leroux et al., 2007).

2.4.3.2. Statistical analysis. Statistical analysis of waste composition and PSD data was achieved using GraphPad Prism version 7.0c for Mac (GraphPad Software Inc.). Descriptive statistics (minimum, maximum, mean and standard deviation) was calculated while assuming a Gaussian distribution and at $p < 0.05$. Furthermore, some datasets were subjected to One-way ANOVA and Tukey's multiple comparison tests.

3. Results and discussions

3.1. Electrical resistivity Tomography (ERT)

3.1.1. ERT on Madesjö open glass dump

Resistivity sections of the two lines at Madesjö glass dump are shown in Fig. 3. The colour progression on the resistivity scales from dark blue to dark red corresponds to resistivity from low to high resistivity. Resistivity over 40,000 Ωm was registered, which fits with the expectation of high glass resistivity (Giancoli, 1998).

The exceptionally high contact resistance at the dump was clearly caused by the highly resistive glass that is exposed on the surface, which can be very problematic for galvanic methods such as ERT. The resistivity contrast among the materials was in fact difficult for the inversion software to handle, which is probably the main reason for the relatively high mean residuals in Table 1 (10.5% and 11.1%). This calls for caution in data interpretation, since the inversion process is known for potential to generate unrealistic variations in model resistivity values, which can lead to over-shooting or under-shooting of the model resistivities on either side of the high contrast transition, uncharacteristic of actual geological features (Jolly et al., 2011). As presented in Table 2, previous ERT studies on landfills have attributed resistivity <70 Ωm (dark to light blue in Fig. 3) to leachate or decomposed wastes, whereas resistivities >348 Ωm (could be 10–2000 Ωm depending on degree of saturation and weathering) have been attributed to demolition waste (Çinar et al., 2015; Boudreault et al., 2010). This interpretation, however, could not be adopted for the Madesjö case since verification TPs were not excavated deep enough to reach beneath the glass pile due to unstable ground posing machine safety risks. Further attemps at literature-based interpretations were hindrered by the high likelihood for introduction of artefacts in the results due to very high discrepancy in resistivity.

Table 2
Parameters for ERT interpretations (modified from Abdulrahman et al., 2016).

Material	Parameter	Value
Granite	SiO_2 content	72.04% (Blatt and Tracy, 1996)[*1]
Glass (silicate)	″	74% (Shelby, 2005)
Granite	Resistivity	1000 – 1 × 10^6 Ωm (Palacky, 1987)
Glass (general)	″	8000 – 6.3 × 10^8 Ωm (CRC Press, 2001)[*2]
Saturated (wet) soil	″	30 – 150 Ωm (Guérin et al., 2004; Dahlin et al., 2010)
Unsaturated (dry) soil	″	>1000 Ωm (Leroux et al., 2007)
Demolition waste	″	348 – 2000 Ωm (Boudreault et al., 2010; Çinar et al., 2015)
Decomposed waste	″	1 – 40 Ωm (Çinar et al., 2015)

[*1] World average.
[*2] Temperature-dependent, although not the value at standard temperature and pressure (STP).

However, the data quality was good, which is judged to be a result of the survey design with separated electrode cables for current transmission and potential measurements in combination with careful field procedures with gel used to enhance electrode-to-ground contact. Therefore, the near-surface data at this site was confidently interpreted both through visual inspection and verification TPs (Fig. 4c).

Near-surface data showed some relatively high resistivity (1000–2500 Ωm) regions indicated by yellow–light orange in Fig. 3. Based on visual inspection of materials heaped on the surface, inspection of the region between 4 and 8 m on line ML_1 revealed demolition waste such as concrete and asbestos roofing sheets as shown in Fig. 4a. This was in line with literature values for demolition waste as presented in Table 2. On both lines (ML_1 and ML_2), the glass heap registered resistivity >8000 Ωm (dark orange to dark red). Resistivity of SiO_2 glass at atmospheric temperature and pressure was not found in literature, although it has been estimated as ranging between 8000–6.3 × 10^8 Ωm depending on temperature (CRC Press, 2001). TPs excavated across the dump (Fig. 4c) verified glass waste as the source of the high resistivity recorded. Although data beneath the glass pile in Fig. 3 was cautiously omitted from inversion results interpretation to avoid mistaking artefacts for actual geological features, one study objective of testing the glass heap to understand 'pure' glass (unburied glass) resistivity was successfully achieved for application at Alsterfors dump where glass was buried.

According to generated fence diagrams in Fig. 3c, the inverted profiles match quite well at the intersections and the data in the 3-D model agree with each other very well, thus confirming a certain level of confidence in the results (Johansson et al., 2016). As such, the Madesjö findings could be reliably used as a 'guide' in identification of buried glass hotspots at Alsterfors dump.

3.1.2. ERT on covered glass hotspots

Resistivity sections for Alsterfors dump are shown in Fig. 5. Lines AL_1, AL_2 and AL_3 are presented in Fig. 5a, b and c respectively. To avoid misinterpretations, knowing that all data comes with a degree of uncertainty in the results, and that the creation of artefacts during the inversion process is a well-known phenomenon (Johansson et al., 2019; Jolly et al., 2011), data interpretation for Alsterfors was mainly based on excavation of verification TPs, literature-based values of material resistivities as presented in Table 2, and resistivity observations from Madesjö glass dump (for glass hotspots). The resistivity scale was aggregated into six categories during interpretation: dark blue zones (<30 Ωm), blue zones (30–70 Ωm), green to dark green zones (60–530 Ωm), light green zones (500–1100 Ωm), yellow to light orange zones (1000–4600 Ωm), and dark orange to dark red zones (>8000 Ωm). The profile images in Fig. 5 provided crucial information about glass hotspots, and guided TP excavations for verification of observed resistivity against set hypotheses. Fig. 5a gives a clear indication of the dump base as shown by the yellow underlying structure (1000–2200 Ωm), which is believed to be part of the bedrock, since the bedrock at the site lies about 3–10 m below the surface (SGU, 2019).

Dark blue zones (<30 Ωm) such as between 28 and 33 m and around 5–8 m depths in Fig. 5b were interpreted as wet zones containing either decomposed waste or leachate or both, as they are

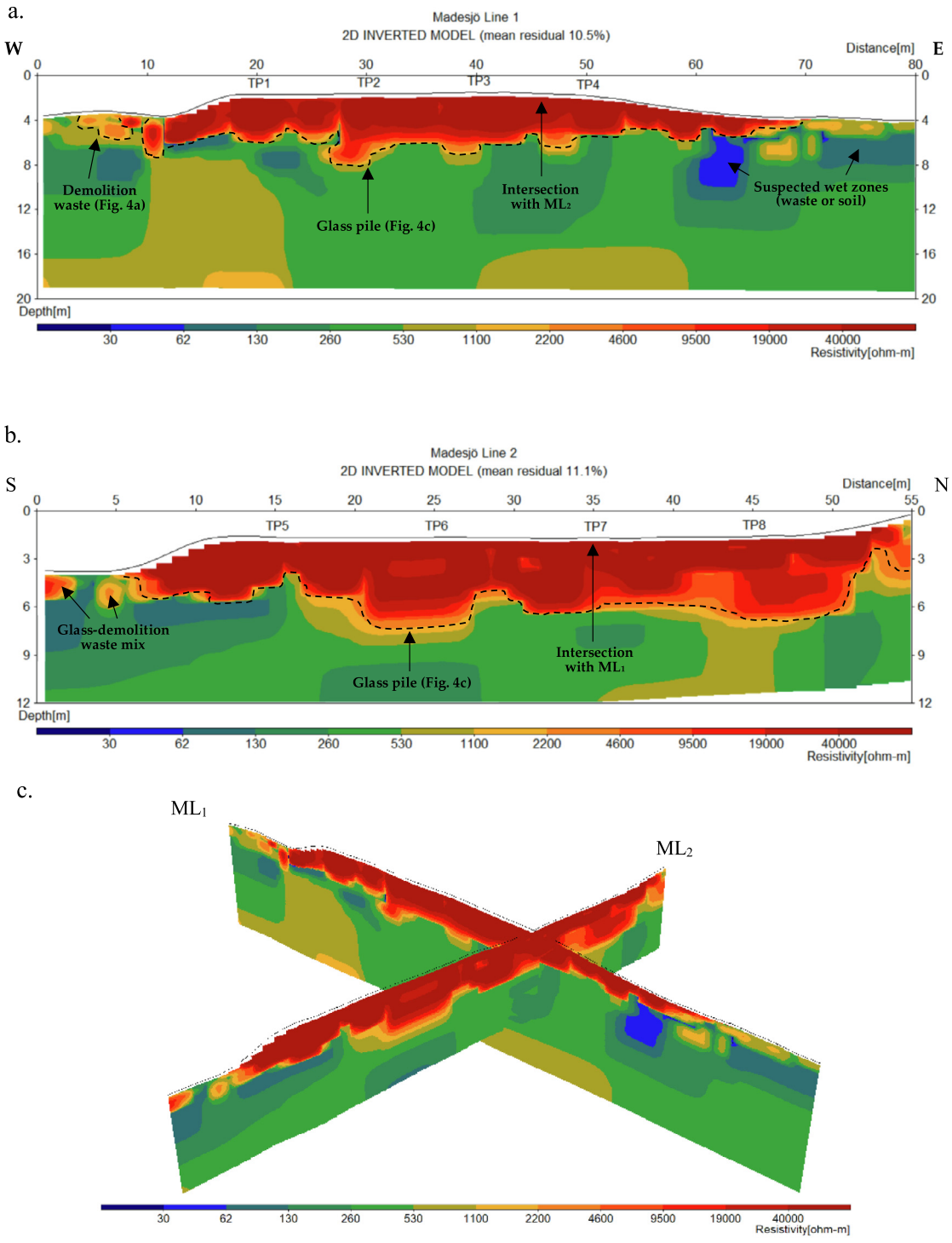

Fig. 3. Resistivity profiles at Madesjö glass dump; (a) line ML_1; (b) line ML_2; and (c) 3-D view of the two lines.

known for resistivity range of 1–40 Ωm (Çınar et al., 2015). The blue to dark green zones (30–130 Ωm) were interpreted as wet soil zones, which have been reported to vary between 30 and 150 Ωm (Guérin et al., 2004; Dahlin et al., 2010). A TP excavated around 69–71 m (TP11) and at 4.5 m depth on AL_2 (Fig. 5b), for example, indicated wet soil as shown in Fig. 6a. On the other hand, lighter green zones (130–530 Ωm), such as between 0 and 28 m and 34–40 m in Fig. 5a, 0–20 m in Fig. 5b, and 13–20 m in Fig. 5c (depth ≥ 5 m) were interpreted as regions of semi-wet soil as evidenced by TP10 on AL_2 (Fig. 5b) and shown in Fig. 6g. Furthermore, the light green to yellow zones (530–2200 Ωm) were interpreted as regions of dry soil as dry soil can register resistivity >1000 Ωm (Leroux et al., 2007). This was verified by TP5 on AL_1 (Fig. 5a) and TP9 on AL_2 (Fig. 5b) as shown in Fig. 6h.

Based on findings from Madesjö glass dump (Fig. 3a), yellow to light orange zones (1000–4600 Ωm) were expected to be demolition waste zones. A TP excavated around such a zone at ≈ 30 m (TP3) in Fig. 5a revealed demolition waste (bricks) with an

Fig. 4. Madesjö glass dump; (a) demolition waste heap at the start of ML_1; (b) start of ML_2 near the stream; (c) TP excavations across the dump.

underlying layer of dry soil as shown in Fig. 6b. Around 66–67 m, there was a downward progression of different resistivity zones (1000–2500 Ωm, then 250–530 Ωm, and 530–1100 Ωm) which TP6 on AL_1 revealed as demolition waste close to the surface, followed by a gentle progression of semi-wet to dry soil as shown in Fig. 6c. However, Fig. 5b also revealed a structure between 28 and 44 m along the line, with resistivity similar to that of excavated demolition waste. In this case, it was clearly not demolition waste but a part of the geological formation of the area, as evidenced by a similar structure underlying the dump in Fig. 5a. This was further revealed by TP9 at 40–42 m on AL_2 (Fig. 5b) as compact and dry soil similar to the one in Fig. 6h.

Glass hotspots were expected to be in the dark orange to dark red zones (>8000 Ωm). There were a number of such zones on all three lines in Fig. 5. On AL_1 (Fig. 5a), three TPs were excavated between 11 and 15 m (TP1), 23–25 m (TP2) and 43–45 m (TP4) and all revealed glass, although it was more abundant at 23–25 m and 43–45 m (Fig. 6d). As such, these two regions were identified as hotspots from which materials for physico-chemical characterisation were sampled as samples S1 and S2 respectively. Although the region between 11 and 15 m was also a glass hotspot, it was not sampled but glass abundance was visually qualified based on amounts of other waste fractions seen during excavations. On AL_2 (Fig. 5b), a TP between 13 and 18 m (TP7) also showed abundant glass waste as shown in Fig. 6e. The region around 4–10 m in Fig. 5b clearly contained abundant glass also as could be seen from the surface, but a verification TP could not be excavated since the region was sloppy with unstable ground, and thus unsafe for the excavator. Similarly, there was abundant glass on the surface around 29–34 m in Fig. 5b, and therefore the highly resistive region beneath was designated as a hotspot. Materials for physico-chemical characterisation were thus sampled from the regions between 13 and 18 m and 29–31 m in Fig. 5b (sample S3). On AL_3 (Fig. 5c), TP12 was excavated at 14–16 m which was another glass hotspot and was thus sampled as S4.

It was noted, however, that the bedrock around the dump showed resistivity similar to some dumped materials. In Fig. 5b, for instance, resistivity >8000 Ωm is progressively registered in the region around 0–34 m and between 10 and 15 m depths. A TP excavated at 26–28 m (TP8) and 1–2 m depths revealed big stones (Fig. 6f) with an underlying bigger rock which the excavator could not remove. It was thus concluded that the bedrock was responsible for resistivity zones >8000 Ωm other than glass hotspots. Alsterfors site has granite bedrock with a moraine soil depth of 3–10 m (SGU, 2019). Granite and soda-lime glass have similar

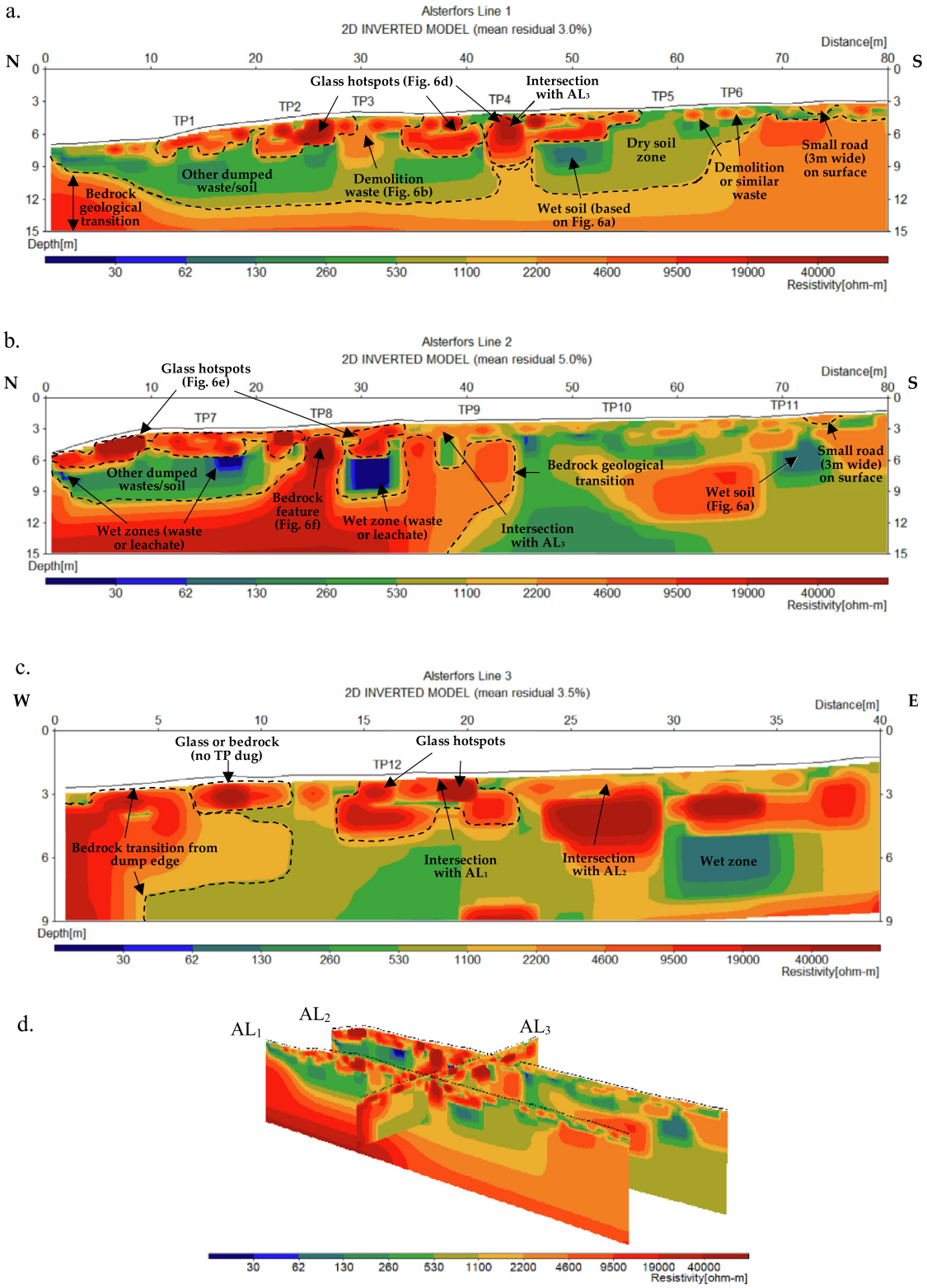

Fig. 5. Resistivity profiles at Alsterfors dump; (a) line AL_1; (b) line AL_2; (c) line AL_3; (d) 3-D view of the three lines.

chemical compositions as shown in Table 2. Granite world average composition is estimated at 72.04% SiO_2 (Blatt and Tracy, 1996) while soda-lime glass comprises about 74% SiO_2 (Shelby, 2005), although soda-lime glass around Swedish glassworks ranged between 55 and 85% SiO_2 (Hermelin and Welander, 1986). Furthermore, granite has a wide resistivity range of 1000–1,000,000 Ωm (Palacky, 1987), implying that different resistivities within this range can be obtained for granite bedrock such as at Alsterfors. For successful identification of glass hotspots, bedrock characteristics must be factored in, meaning that in sites with bedrock that do not possess glass characteristics, hotspots could be identified much easier.

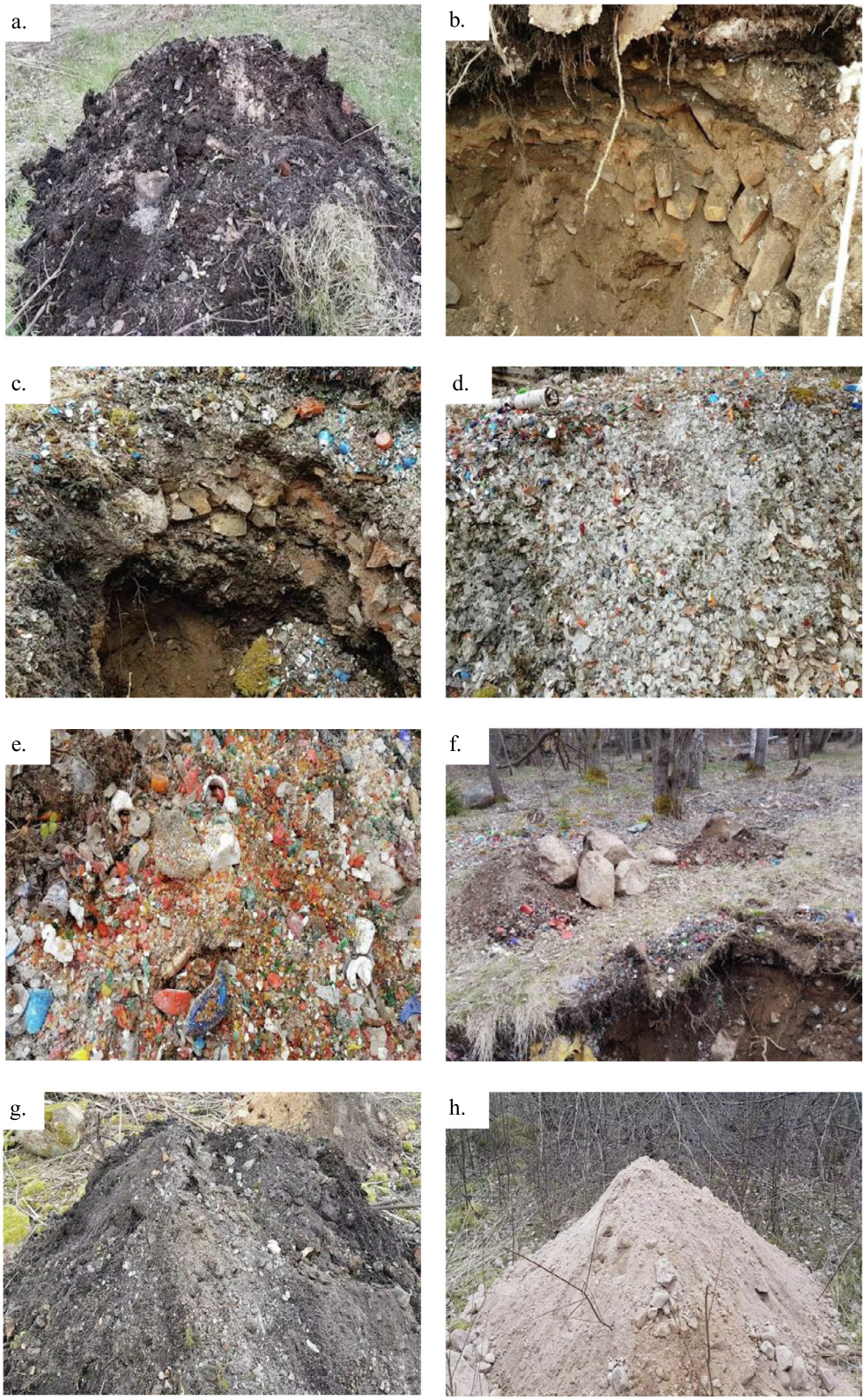

Fig. 6. Results of TP excavations at Alsterfors dump; (a) wet soil from AL_2; (b) demolition waste from AL_1; (c) demolition waste profile with semi-wet soil beneath on AL_1; (d) glass waste from a hotspot on AL_1; (e) glass waste from a hotspot on AL_2; (f) rocks from an initially suspected hotspot on AL_2; (g) semi-wet soil from AL_2; (h) compact, dry soil with stones from AL_2.

Although some glass hotspots were successfully identified, more verifications were impeded by the small number of TPs as well as lack of trench-digging along the lines, which could give more information. This particular limitation was due to time and other resource constraints. In addition, 2-D ERT only produces vertical cross sections of a dump, which tends to limit full understanding of dumped material quantities. The use of 3-D ERT or complementing different geophysical methods instead could give

more information, since each method has its own strengths and weaknesses (Reynolds, 2011). Furthermore, since unused raw material batches were also dumped during production years (Uddh-Söderberg et al., 2019), there could be a risk of mistaking the dumped batches for glass hotspots as they are expected to have similar properties. However, such was not encountered in the current investigation. Regardless of the limitations, a high level of confidence in the results was also displayed at Alsterfors dumpsite for the near-surface materials which was the target of the investigation since glass dumps are inherently shallow. Confidence in the results was also evidenced by the matching inverted profiles at intersections and agreement of data in the 3-D visualisation in Fig. 5d.

3.1.3. Hotspot material particle size distribution

The particle sizes of the hotspot samples (S1, S2, S3 and S4) was obtained as shown in Fig. 7. By means, the course fraction (CF) was dominating (38.3 ± 13.8%) followed by the medium (31.3 ± 9.5%) and fine (28.3 ± 5.4%) fractions as presented in Fig. 7a. According to a One-way ANOVA ($p < 0.05$) the differences among the means were not statistically significant. The high standard deviations can be attributed to influence from unusually bigger particles in a size category especially in coarser categories (Kaartinen et al., 2013). From previous landfill mining (LFM) investigations, CF have ranged between 24 and 59.2%, medium fraction (MF) between 21.8 and 29.9%, and FF between 14.8 and 73.6%, depending on study settings, waste type and age (Hogland et al., 2004; Jani et al., 2016; Mönkäre et al., 2016; Mutafela et al., 2019, 2020). A challenge with comparing different study findings is that each study site is unique due to heterogeneity. However, particle sizes of different studies could be compared using PSD regardless of the study settings. Fig. 7b shows PSD results based on particles passing through a sieve mesh. The observed 45 ± 9% for particles <20 mm, for instance, is comparable with the 45 ± 7% at Kuopio MSW landfill, while the observed 44% for particles <4 mm is also comparable with the 44%–57% range at the same landfill in Finland (Kaartinen et al., 2013; Mönkäre et al., 2016).

PSD influences moisture content, which in turn influences resistivity distribution in subsurface structures as explained in Section 3.1.5. The bigger the particle sizes, the lower the water retention capacity, and vice versa. In terms of materials recycling, excavated material particle sizes are important in identification of optimum material sorting techniques (Spooren et al., 2013) and relevant waste processing technologies (Jani et al., 2016). Furthermore, PSD will be key for future recycling-oriented LFM activities for separation of FF into exploitable resources to avoid or minimise materials re-landfilling (Parrodi et al., 2018).

3.1.4. Hotspot material waste composition

Results of hand-sorting of the material fractions are shown in Fig. 7c. Glass fraction was dominating (87.2%) followed by soil (6.6%), demolition (4.1%), residual (1.3%) and lastly organic (0.8%) fractions. Unusually high standard deviations were observed in some fractions due to the long ranges in results. For instance, demolition fraction ranged between 0 and 61.5% while soil ranged between 0 and 44.3%. A One-way ANOVA ($p < 0.05$) of the results indicated that there was a statistically significant difference among the means. According to Turkey's multiple comparisons test (95% confidence interval), glass differed significantly from other fractions, while there were no statistically significant differences among all other means. The results clearly indicate the presence of glass hotspots as confirmed from hand-sorting of the material fractions from the four samples. The results further suggest that while there are sections in the dump with mixed material fractions as established through ERT models and confirmed by TP excavations, some sections (hotspots) contain materials that could be readily available for recycling processes if excavated carefully. However, these results do not suggest a general pattern among different glass dumps, as this may depend on each factory's disposal practice. The high resistivities registered in the ERT models around initially suspected hotspots are thus confirmed by the results (87.2% glass).

3.1.5. Moisture content

Moisture content varied between the two sites (Alsterfors and Madesjö) as well as material types (glass hotspots and soil) at Alsterfors. It was highest in Alsterfors soil samples at 24.9 ± 4.3% followed by Alsterfors glass hotspot samples at 5.7 ± 1.6% and lastly Madesjö glass samples at 3.1 ± 0.6%. Moisture content in landfills is influenced by waste composition, type, properties and local climatic conditions (Hull et al., 2005). The observed differences can thus be explained by these factors, including drainage characteristics (Quaghebeur et al., 2013). Moisture content of excavated waste is an important factor in evaluation of valorisation and treatment alternatives (Hull et al., 2005; Quaghebeur et al., 2013). As such, it has been extensively studied in different LFM studies where it ranged between 22 and 66%, which is comparable to the Alsterfors soil part in this study (Bhatnagar et al., 2017; Hogland

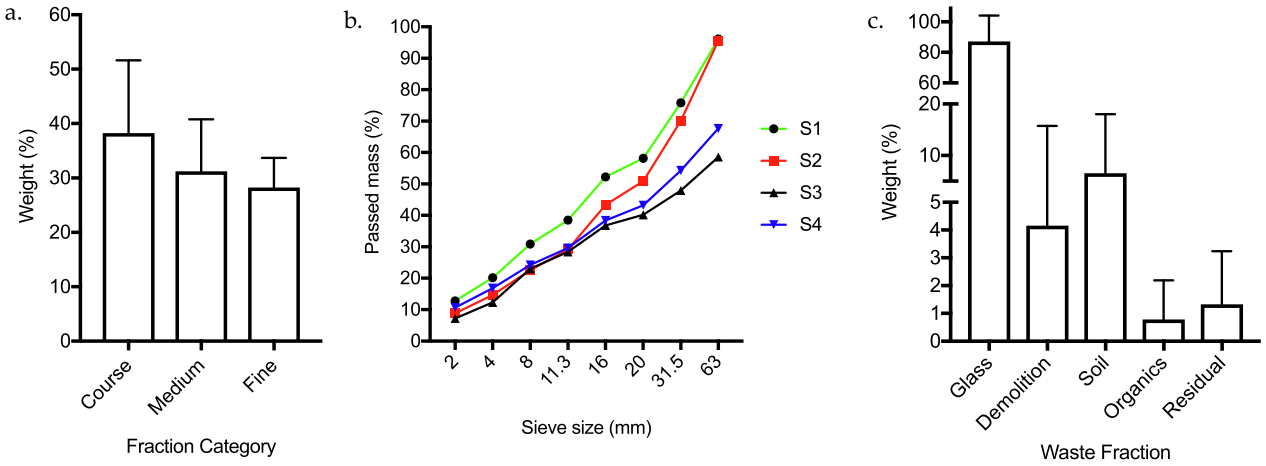

Fig. 7. (a) Distribution of fraction categories from all samples (n = 4); (b) particle size distribution averages presented in passed mass (%); (c) waste fractions of excavated hotspot materials.

et al., 2004; Hull et al., 2005; Jani et al., 2016; Mönkäre et al., 2016; Quaghebeur et al., 2013).

The importance of moisture content in the current study, however, is in its influence on subsurface resistivity, since it exerts the dominant control over resistivity distribution in landfill environments (Bernstone et al., 2000). Moisture content is inversely proportional to resistivity of subsurface materials. For instance, igneous and metamorphic rocks have higher resistivities than sedimentary rocks given the latter's higher porosity, and thus higher water content (Pomposiello et al., 2012). Archie's empirical equation (Archie, 1942) best describes the relationship:

$$\rho = a\rho_w n^m s^l \quad (1)$$

where ρ = rock or soil resistivity, a = tortuosity or lithology constant, ρ_w = pore water resistivity, n = porosity, m = cementation exponent, s = degree of saturation, and l = saturation exponent (Glover, 2016). Thus, resistivity is largely dependent on the moisture content, pore water resistivity, and how the pore water is distributed in the mineral i.e. porosity, degree of cementation, degree of saturation, and fracture state (Clayton et al., 1995). These factors are in turn important in interpretation of the obtained electrical resistivity models.

3.1.6. Trace element contents

The trace element contents of the sampled waste from Alsterfors dump glass hotspots and Madesjö glass dump are shown in Table 3 in comparison with Swedish Environmental Protection Agency (SEPA) limits for hazardous waste (Avfall Sverige, 2007). The elements As, Cd, Pb and Zn were in hazardous amounts while Ba, Cu and Sb were lower than their respective SEPA limits. The hazardous amounts of some of the elements correspond to their frequent uses in glass production. As_2O_3 was used as a refining and decolourising agent, CdS as a colouring agent and Pb_3O_4 as a glass network stabiliser and modifier (Hermelin and Welander, 1986). The variations in concertation of Pb especially in Alsterfors glass samples could be attributed to little use of Pb since the factory did not primarily produce Pb crystal glass. Furthermore, the use of Pb as a core component of crystal glass was only enacted by an EU directive in 1969 (European Community, 1969), towards the final years of the factory. The results also imply that sample S4 may have contained some Pb crystal glass.

The high contents of As, Cd, Pb and Zn in hotspot glass could benefit metal extraction processes, although no economic feasibility analysis was done to assess potential contribution of such secondary metal sources to the high global demand. Estimations of possible economic gains in view of recycling as secondary raw materials could be useful. Furthermore, since the 2-D ERT only focuses on single depth profiles that do not give full indication of the material volumes in a whole dump, incorporation of 3-D ERT or different complementary geophysical methods is recommended in the effort to achieve economic feasibility assessments.

4. Conclusions

ERT was conducted at two old glass dumps (open and buried glass) to identify glass hotspots for excavation and later use as sources of secondary raw materials. Despite challenging site conditions, with exceptionally high contact resistances at one of the sites, good quality data was achieved, thanks to suitable survey design and careful field procedures. Identification of glass hotspots in the buried glass dump was guided by the ERT results from the open glass dump and was based on sharp contrasts in resistivity between glass and other materials. Regions of high resistivity (>8000 Ωm) were confirmed through TP excavations as glass hotspots. Physico-chemical characterisation of hotspot materials, indicating mean waste composition of 87.2% glass (up to 99% in some samples), further confirmed glass hotspots and thus the potential for ERT to identify them. Furthermore, careful excavation of TPs with ERT as the pre-excavation guide indicated the potential for obtaining 'clean' glass for recycling purposes, which would be challenging to obtain through random, uncoordinated excavations.

The study, however, encountered some limitations that require caution during data acquisition and interpretation in glass waste dumps. Firstly, the similarities in resistivity between Granite bedrock and crystal glass present the risk of misinterpretation, especially in a site like Alsterfors where both lie close to the surface. This, however, would not be a big limitation in sites with deep-lying and different bedrock types. Secondly, the high resistivity contrasts are prone to introduce artefacts in the results, which may further increase the degree of uncertainty with depth. Furthermore, at sites with complex variation in resistivity the 3-D character of the variation will lead to artefacts in 2-D ERT results, so called 3-D effects. This can be handled by using a 3-D ERT approach, e.g. by measuring a number of parallel 2-D ERT lines and merging the data to a 3-D data set before inversion, which prevents this type of artefacts but requires more data to be collected. It is recommended, therefore, that a modelling study about variation of resistivity with depth and introduction of artefacts (their nature, magnitude and impact) in such sites be conducted, assessing 2-D as well as 3-D ERT approaches, in order to find a suitable trade-off between quality of results and survey cost.

Nevertheless, given the inherent shallowness of glass waste dumps, it is concluded that ERT is applicable since uncertainty is considerably reduced near the surface. ERT could thus be a useful non-destructive technique towards obtaining more homogeneous buried glass and other wastes from LFM for use as secondary raw material sources in metal extraction and other waste recycling techniques while eliminating complicated and often costly waste sorting mechanisms. These findings could contribute to the effort for decontamination of such old dumpsites with integration of sustainable material recovery techniques for the circular economy.

Table 3
Trace element concentrations of sampled waste glass compared with Swedish EPA limits for hazardous waste (Avfall Sverige, 2007).

Element (mg kg^{-1})	Madesjö Glass	Alsterfors Glass S1	Alsterfors Glass S2	Alsterfors Glass S3	Alsterfors Glass S4	Swedish EPA limits for hazardous waste
As*	13,138 (4 5 1)	2636 (34)	3102 (36)	4468 (43)	4781 (58)	1000
Ba	1221 (46)	860 (34)	522 (35)	411 (26)	376 (27)	10,000
Cd*	394 (25)	443 (10)	430 (11)	522 (11)	647 (14)	100
Cu	551 (44)	125 (9)	456 (13)	369 (11)	769 (18)	2500
Pb*	245,822 (3494)	5929 (60)	1315 (18)	2737 (29)	11,470 (1 4 2)	2500
Sb	4233 (1 4 1)	243 (14)	571 (19)	1022 (21)	1065 (23)	10,000
Zn*	4032 (1 0 1)	7020 (72)	8108 (90)	14,320 (1 2 5)	10,882 (1 0 7)	2500

Elements exceeding at least one limit indicated by (*); Values in brackets represent standard deviations.

Acknowledgements

We are grateful to AB Kosta Kapell, Nybro Municipality and Ragn Sells AB for support and facilitation of sampling permits. We would also like to thank Mr. David Silfwersvärd (Linnaeus University) for assistance during geophysical mapping field work. Furthermore, the authors are thankful for the contribution given by the reviewers, which improved the quality of the manuscript substantially.

Funding

This research was funded by the Swedish Agency for Innovation Systems (Vinnova). Grant code: 2017-03244.

Declaration of Competing Interest

The authors declare no conflict of interests.

References

Abdulrahman, A., Nawawi, M., Saad, R., Abu-Rizaiza, A.S., Yusoff, M.S., Khalil, A.E., Ishola, K.S., 2016. Characterization of active and closed landfill sites using 2D resistivity/IP imaging: case studies in Penang, Malaysia. Environ. Earth Sci. 75 (4), 347. https://doi.org/10.1007/s12665-015-5003-5.

Archie, G.E., 1942. The electrical resistivity log as an aid in determining some reservoir characteristics. Trans. AIME 146 (01), 54–62. https://doi.org/10.2118/942054-G.

Augustsson, A., Åström, M., Bergbäck, B., Elert, M., Höglund, L.O., Kleja, D.B., 2016. High metal reactivity and environmental risks at a site contaminated by glass waste. Chemosphere 154, 434–443. https://doi.org/10.1016/j.chemosphere.2016.03.125.

Sverige, Avfall, 2007. Uppdaterade bedömningsgruder för förorenade massor. Malmö (In Swedish).

Beerkens, R., Kers, G., van Santen, E., 2010. Recycling of Post-Consumer Glass: Energy Savings, CO2 Emission Reduction, Effects on Glass Quality and Glass Melting. Paper presented at the 71st Conference on Glass Problems. State University, The Ohio.

Bernstone, C., Dahlin, T., Ohlsson, T., Hogland, H., 2000. DC-resistivity mapping of internal landfill structures: two pre-excavation surveys. Environ. Geol. 39 (3), 360–371. https://doi.org/10.1007/s002540050015.

Bhatnagar, A., Kaczala, F., Burlakovs, J., Kriipsalu, M., Hogland, M., Hogland, W., 2017. Hunting for valuables from landfills and assessing their market opportunities A case study with Kudjape landfill in Estonia. Waste Manage. Res. 35 (6), 627–635. https://doi.org/10.1177/0734242X17697816.

Blatt, H., Tracy, R.J., 1996. Petrology: Igneous, Sedimentary and Metamorphic. W.H. Freeman and Company, New York.

Boudreault, J.-P., Dubé, J.-S., Chouteau, M., Winiarski, T., Hardy, É., 2010. Geophysical characterization of contaminated urban fills. Eng. Geol. 116 (3), 196–206. https://doi.org/10.1016/j.enggeo.2010.09.002.

British Geological Survey. 2015. Current Supply Risk for Chemical Elements or Element Groups which are of Economic Value. Retrieved from https://www.bgs.ac.uk/mineralsUK/statistics/riskList.html.

Çınar, H., Altundaş, S., Ersoy, E., Bak, K., Bayrak, N., 2015. Application of two geophysical methods to characterize a former waste disposal site of the Trabzon-Moloz district in Turkey. Environ. Earth Sci. 75 (1), 52. https://doi.org/10.1007/s12665-015-4839-z.

Clayton, C.R.I., Matthews, M.C., Simons, N.E., 1995. Subsurface exploration: engineering geophysics. In: Site Investigation. Wiley Blackwell, Oxford, pp. 1–68.

CRC Press, 2001. CRC-Material Science and Engineering Handbook. In: Shackelford, J.F., Alexander, W. (Eds.), Engineering Handbook, 3rd ed., vol. 1. CRC Press, Boca Raton.

Dahlin, T., Leroux, V., 2012. Improvement in time-domain induced polarization data quality with multi-electrode systems by separating current and potential cables. Near Surf. Geophys. 10 (6), 545–565. https://doi.org/10.3997/1873-0604.2012028.

Dahlin, T., Rosqvist, H., Leroux, V., 2010. Resistivity-IP mapping for landfill applications. First Break 28 (8).

Dahlin, T., Zhou, B., 2004. A numerical comparison of 2D resistivity imaging with 10 electrode arrays. Geophys. Prospect. 52 (5), 379–398. https://doi.org/10.1111/j.1365-2478.2004.00423.x.

Dahlin, T., Zhou, B., 2006. Multiple-gradient array measurements for multichannel 2D resistivity imaging. Near Surf. Geophys. 4 (2), 113–123. https://doi.org/10.3997/1873-0604.2005037.

Dumont, G., Robert, T., Marck, N., Nguyen, F., 2017. Assessment of multiple geophysical techniques for the characterization of municipal waste deposit sites. J. Appl. Geophys. 145, 74–83. https://doi.org/10.1016/j.jappgeo.2017.07.013.

Duncan, A., 1995. Orrefors Glass. Antique Collectors' Club Ltd, Woodbridge, England.

Edjabou, M.E., Jensen, M.B., Götze, R., Pivnenko, K., Petersen, C., Scheutz, C., Astrup, T.F., 2015. Municipal solid waste composition: Sampling methodology, statistical analyses, and case study evaluation. Waste Manage. 36, 12–23. https://doi.org/10.1016/j.wasman.2014.11.009.

European Community, 1969. Council Directive 69/493/EEC of 15 December 1969 on the approximation of the laws of the Member States relating to crystal glass. Retrieved from https://publications.europa.eu/en/publication-detail/-/publication/5676d686-f732-410f-af45-142245959a8b/language-en.

Giancoli, D.C., 1998. Physics: principles with applications. Prentice Hall, Upper Saddle River, N.J..

Glover, P.W.J., 2016. Archie's law – a reappraisal. Solid Earth 7 (4), 1157–1169. https://doi.org/10.5194/se-7-1157-2016.

Guérin, R., Munoz, M.L., Aran, C., Laperrelle, C., Hidra, M., Drouart, E., Grellier, S., 2004. Leachate recirculation: moisture content assessment by means of a geophysical technique. Waste Manage. 24 (8), 785–794. https://doi.org/10.1016/j.wasman.2004.03.010.

Hermelin, C.F., Welander, E., 1986. Glasboken - Historia, teknik och form. Centraltryckeriet AB, Borås (In Swedish).

Hogland, W., Hogland, M., Marques, M., 2010. Enhanced Landfill Mining: Material recovery, energy utilisation and economics in the EU (Directive) perspective. In: Paper presented at the ELFM symposium - enhanced landfill mining and the transition to sustainable materials management. Houthalen-Helchteren, Belgium.

Hogland, W., Marques, M., Nimmermark, S., 2004. Landfill mining and waste characterization: a strategy for remediation of contaminated areas. J. Mater. Cycles Waste Manage. 6 (2), 119–124. https://doi.org/10.1007/s10163-003-0110-x.

Höglund, L.O., Fanger, G., Yesilova, H., 2007. Slutrapport – Glasbruksprojektet 2006–2007. Kalmar (In Swedish).

Hsu, H.-L., Yanites, B.J., Chen, C.-C., Chen, Y.-G., 2010. Bedrock detection using 2D electrical resistivity imaging along the Peikang River, central Taiwan. Geomorphology 114 (3), 406–414. https://doi.org/10.1016/j.geomorph.2009.08.004.

Hull, R.M., Krogmann, U., Strom, P.F., 2005. Composition and characteristics of excavated materials from a New Jersey landfill. J. Environ. Eng. 131 (3), 478–490. https://doi.org/10.1061/(ASCE)0733-9372(2005)131:3(478).

Jani, Y., Hogland, W., 2014. Waste glass in the production of cement and concrete – A review. J. Environ. Chem. Eng. 2 (3), 1767–1775. https://doi.org/10.1016/j.jece.2014.03.016.

Jani, Y., Hogland, W., 2017. Reduction-melting extraction of trace elements from hazardous waste glass from an old glasswork's dump in the southeastern part of Sweden. Environ. Sci. Pollut. Res. 24 (34), 26341–26349. https://doi.org/10.1007/s11356-017-0243-4.

Jani, Y., Hogland, W., 2018. Chemical extraction of trace elements from hazardous fine fraction at an old glasswork dump. Chemosphere 195, 825–830. https://doi.org/10.1016/j.chemosphere.2017.12.142.

Jani, Y., Kaczala, F., Marchand, C., Hogland, M., Kriipsalu, M., Hogland, W., Kihl, A., 2016. Characterisation of excavated fine fraction and waste composition from a Swedish landfill. Waste Manage. Res. 34 (12), 1292–1299. https://doi.org/10.1177/0734242X16670000.

Johansson, S., Lindskog, A., Fiandaca, G., Dahlin, T., 2019. Spectral induced polarization of limestones: time domain field data, frequency domain laboratory data and physicochemical rock properties. Geophys. J. Int. 220 (2), 928–950. https://doi.org/10.1093/gji/ggz504.

Johansson, S., Sparrenbom, C., Fiandaca, G., Lindskog, A., Olsson, P.-I., Dahlin, T., Rosqvist, H., 2016. Investigations of a Cretaceous limestone with spectral induced polarization and scanning electron microscopy. Geophys. J. Int. 208 (2), 954–972. https://doi.org/10.1093/gji/ggw432.

Jolly, J.M., Beaven, R.P., Barker, R.D., 2011. Resolution of electrical imaging of fluid movement in landfills. Proc. ICE – Waste Resource Manage. 164, 79–96. https://doi.org/10.1680/warm.2011.164.2.79.

Kaartinen, T., Sormunen, K., Rintala, J., 2013. Case study on sampling, processing and characterization of landfilled municipal solid waste in the view of landfill mining. J. Cleaner Prod. 55, 56–66. https://doi.org/10.1016/j.jclepro.2013.02.036.

Kaczala, F., Mehdinejad, M.H., Lääne, A., Orupõld, K., Bhatnagar, A., Kriipsalu, M., Hogland, W., 2017. Leaching characteristics of the fine fraction from an excavated landfill: physico-chemical characterization. J. Mater. Cycles Waste Manage. 19 (1), 294–304. https://doi.org/10.1007/s10163-015-0418-3.

Länsstyrelsen Kalmar, 2012. Prioriterade områden i Kalmar län - Madesjötippen. (In Swedish).

Länsstyrelsen Kalmar, 2019. Prioriteringslista över förorenade områden i Kalmar län. (In Swedish).

Länsstyrelsen Kronoberg, 2018. Prioriterade områden i Kronobergs län - Alsterfors glasbruk. (In Swedish).

Leroux, V., Dahlin, T., Svensson, M., 2007. Dense resistivity and induced polarization profiling for a landfill restoration project at Härlöv, Southern Sweden. Waste Manage. Res. 25 (1), 49–60. https://doi.org/10.1177/0734242X07073668.

Loke, M.H., 1999. Electrical imaging surveys for environmental and engineering studies. A practical guide to 2-D and 3-D surveys 2, 67.

Loke, M.H., Acworth, I., Dahlin, T., 2003. A comparison of smooth and blocky inversion methods in 2D electrical imaging surveys. Explor. Geophys. 34 (3), 182–187. https://doi.org/10.1071/EG03182.

Loke, M.H., Wilkinson, P.B., Chambers, J.E., 2010. Fast computation of optimized electrode arrays for 2D resistivity surveys. Comput. Geosci. 36 (11), 1414–1426. https://doi.org/10.1016/j.cageo.2010.03.016.

Mönkäre, T.J., Palmroth, M.R.T., Rintala, J.A., 2016. Characterization of fine fraction mined from two Finnish landfills. Waste Manage. 47, 34–39. https://doi.org/10.1016/j.wasman.2015.02.034.

Mutafela, R., Kaczala, F., Jani, Y., Aid, G., Hogland, W., 2018. Methods for Investigation of Old Glass Waste Dumpsites. In: Paper presented at the 4th International Symposium on Enhanced Landfill Mining. Mechelen, Belgium.

Mutafela, R.N., Marques, M., Jani, Y., Kriipsalu, M., Hogland, W., 2019. Physico-chemical characteristics of fine fraction materials from an old crystal glass dumpsite in Sweden. Chem. Ecol. 35 (9), 877–890. https://doi.org/10.1080/02757540.2019.1648442.

Mutafela, R.N., Mantero, J., Jani, Y., Thomas, R., Holm, E., Hogland, W., 2020. Radiometrical and physico-chemical characterisation of contaminated glass waste from a glass dump in Sweden. Chemosphere 241,. https://doi.org/10.1016/j.chemosphere.2019.124964 124964.

Palacky, G.J., 1987. Resistivity Characteristics of Geologic Targets. In: Nabighian, M. N. (Ed.), Electromagnetic Methods in Applied Geophysics: Volume 1, Theory. Society of Exploration Geophysicists, pp. 52–129.

Parrodi, J.C.H., Höllen, D., Pomberger, R., 2018. Characterization of fine fractions from landfill mining: A review of previous investigations. Detritus 2, 46–62. https://doi.org/10.31025/2611-4135/2018.13663.

Pomposiello, C., Dapeña, C., Favetto, A., Boujon, P., 2012. Application of geophysical methods to waste disposal studies. In: Yu, X.-Y. (Ed.), Municipal and Industrial Waste Disposal. InTech.

Powers, C.J., Wilson, J., Haeni, F.P., Johnson, C.D., 1999. Surface-geophysical investigation of the University of Connecticut landfill, Storrs, Connecticut (99-4211). Retrieved from.

Quaghebeur, M., Laenen, B., Geysen, D., Nielsen, P., Pontikes, Y., Van Gerven, T., Spooren, J., 2013. Characterization of landfilled materials: screening of the enhanced landfill mining potential. J. Cleaner Prod. 55, 72–83. https://doi.org/10.1016/j.jclepro.2012.06.012.

Reynolds, J.M., 2011. An Introduction to Applied and Environmental Geophysics. John Wiley & Sons, West Sussex.

SGU, 2019. SGU Map Viewer – Open Geological Information. The Geological Survey of Sweden, Uppsala.

Shelby, J.E., 2005. Introduction to Glass Science and Technology. The Royal Society of Chemistry, Cambridge.

Spooren, J., Van den Bergh, K., Nielsen, P., Quaghebeur, M., 2013. Landfilled fine grained mixed industrial waste: metal recovery. Acta Metallurgica Slovaca 19 (3), 160–169. https://doi.org/10.12776/ams.v19i3.157.

Uddh-Söderberg, T., Berggren Kleja, D., Åström, M., Jarsjö, J., Fröberg, M., Svensson, A., Augustsson, A., 2019. Metal solubility and transport at a contaminated landfill site – From the source zone into the groundwater. Sci. Total Environ. 668, 1064–1076. https://doi.org/10.1016/j.scitotenv.2019.03.013.

UN. 2017. World population projected to reach 9.8 billion in 2050, and 11.2 billion in 2100. Retrieved from https://www.un.org/development/desa/en/news/population/world-population-prospects-2017.html.

UNEP, 2011. Decoupling natural resource use and environmental impacts from economic growth. UNEP/Earthprinst.

UNEP, 2013. Metals Recycling: Opportunities, Limits, Infrastructure. UNEP/Earthprint.

Wang, T.-P., Chen, C.-C., Tong, L.-T., Chang, P.-Y., Chen, Y.-C., Dong, T.-H., Cheng, S.-N., 2015. Applying FDEM, ERT and GPR at a site with soil contamination: A case study. J. Appl. Geophys. 121, 21–30. https://doi.org/10.1016/j.jappgeo.2015.07.005.

Zarroca, M., Linares, R., Velásquez-López, P.C., Roqué, C., Rodríguez, R., 2015. Application of electrical resistivity imaging (ERI) to a tailings dam project for artisanal and small-scale gold mining in Zaruma-Portovelo, Ecuador. J. Appl. Geophys. 113, 103–113. https://doi.org/10.1016/j.jappgeo.2014.11.022.